AMERICAN COLLEGE
of RHEUMATOLOGY
Empowering Rheumatology Professionals

Using Transitional Changes on High-Resolution Computed Tomography to Monitor the Impact of Cyclophosphamide or Mycophenolate Mofetil on Systemic Sclerosis–Related Interstitial Lung Disease

Grace Hyun J. Kim,[1] [iD]   Donald P. Tashkin,[2] Pechin Lo,[2] Matthew S. Brown,[2] Elizabeth R. Volkmann,[2] [iD]
David W. Gjertson,[3] Dinesh Khanna,[4] [iD]   Robert M. Elashoff,[2] Chi-Hong Tseng,[2] Michael D. Roth,[2] and
Jonathan G. Goldin[2]

Objective. To examine changes in the extent of specific patterns of interstitial lung disease (ILD) as they transition from one pattern to another in response to immunosuppressive therapy in systemic sclerosis–related ILD (SSc-ILD).

Methods. We evaluated changes in the quantitative extent of specific lung patterns of ILD using volumetric high-resolution computed tomography (HRCT) scans obtained at baseline and after 2 years of therapy in patients treated with either cyclophosphamide (CYC) for 1 year or mycophenolate mofetil (MMF) for 2 years in Scleroderma Lung Study II. ILD patterns included lung fibrosis, ground glass, honeycombing, and normal lung. Net change was calculated as the difference in the probability of change from one ILD pattern to another. Wilcoxon's signed rank test was used to compare the changes.

Results. Forty-seven and 50 patients had baseline and follow-up scans in the CYC and MMF groups, respectively. Mean net improvements reflecting favorable changes from one ILD pattern to another in the whole lung in the CYC and MMF groups, respectively, were as follows: from lung fibrosis to a normal lung pattern, 21% and 19%; from a ground-glass pattern to a normal lung pattern, 30% and 28%; and from lung fibrosis to a ground-glass pattern, 5% and 0.5%. The mean overall improvement in transitioning from a ground-glass pattern or lung fibrosis to a normal lung pattern was significant for both treatments (all $P < 0.001$).

Conclusion. Significantly favorable transitions from both ground-glass and lung fibrosis ILD patterns to a normal lung pattern were observed in patients undergoing immunosuppressive treatment for SSc-ILD, suggesting the usefulness of examining these transitions for insights into the underlying pathobiology of treatment response.

INTRODUCTION

Systemic sclerosis (SSc; scleroderma) is a complex life-threatening autoimmune disease associated with tissue fibrosis. SSc-related interstitial lung disease (SSc-ILD) is common and is the leading cause of mortality in SSc (1–3). The majority of patients with SSc develop parenchymal abnormalities on high-resolution computed tomography (HRCT) of the chest, while only ~40% develop significant ventilatory restriction (forced vital capacity percent predicted [FVC%] <75%) and 10–15% develop severe

restrictive abnormality (FVC% <50%) (3,4). Most SSc patients develop ILD within the first 5–10 years of disease onset, and those with more severe restrictive abnormality are at greatest risk of progression to respiratory failure and death (5).

HRCT alterations characteristic of SSc-ILD include reticulations with architectural distortion (representing fibrosis); ground-glass opacity, defined as opacity through which normal lung markings may be visualized, representing either inflammation and/or early fibrosis; and, to a lesser extent, honeycombing (cystic air spaces with fibrous walls) (6). The combination of these elements represents the total burden of ILD that can broadly be assessed either visually or quantitatively using image analysis software (6–15). Along with pulmonary function tests, the radiographic extent of disease in patients with SSc-ILD is important for diagnosis, the staging of disease severity, and the assessment of changes during follow-up (16,17). Furthermore, changes in the extent of fibrosis (reticulations) assessed in the whole lung or in the most involved lobe either visually or by computer-aided quantitative analysis occur in parallel with changes in pulmonary function test findings in response to treatment with oral cyclophosphamide (CYC) or placebo over a 1-year period (18–20).

We previously reported transitional changes in the pixel-based quantitative extent of disease from one ILD pattern to another on paired HRCT scans obtained 1 year apart in 83 patients with SSc-ILD who participated in a trial of oral CYC (n = 41) versus placebo (n = 42) administered for 1 year (Scleroderma Lung Study I [SLS I]) (20). We found significantly greater changes over the 1-year course of the study from a fibrotic or a ground-glass pattern to a normal pattern than the reverse in the 41 CYC-treated patients, whereas the placebo-treated patients tended to show changes in the opposite direction. A limitation of that prior study was that the scans were nonvolumetric and were based on matching arbitrarily designated zones, thereby precluding the ability to quantitate the extent of ILD based on matching voxels and to segment the lung into lobes for analysis of voxelwise transitions within specific lobes.

To further explore transitional changes in the HRCT patterns of SSc-ILD as a sensitive and specific metric of disease progression and treatment response in patients with SSc-ILD, we now present the results of individual voxelwise changes over 2 years in HRCT patterns of quantitative lung fibrosis (QLF), quantitative ground-glass opacity (QGG), and quantitative normal lung (QNL) in both the whole lung and the most severely affected lobe in participants in SLS II, a multicenter trial of oral CYC versus mycophenolate mofetil (MMF) in patients with symptomatic SSc-ILD (21).

MATERIALS AND METHODS

Patient selection. Ninety-seven patients with symptomatic SSc-ILD (25 men and 72 women with a mean ± SD FVC% of 66.3 ± 8.9% and diffusing capacity for carbon monoxide percent predicted [DLco%] of 55.0 ± 13.1%) who participated in the 14-center SLS II and successfully underwent HRCT scans at screening ("baseline") and 2 years following randomization were evaluated for the purpose of this exploratory outcome analysis. Eligible participants were randomly assigned to receive, in a double-blind manner, either oral CYC (titrated to up to 2 mg/kg per day, as tolerated) for 1 year, followed by placebo for an additional year, or MMF (titrated to 1,500 mg twice daily, as tolerated) for 2 years. Full details concerning the SLS II methodology, including eligibility criteria, have been reported previously (21).

Measurements of FVC, DLco, total lung capacity (TLC), dyspnea (Mahler baseline dyspnea index [BDI] and transition dyspnea index [TDI]) (22), and skin thickness score (modified Rodnan skin thickness score [MRSS]) (23) were performed at baseline and repeated every 3 months (FVC, DLco, and MRSS) or every 6 months (TLC and TDI) for 2 years (22,23). The study was approved by the local institutional review board of each participating institution. All radiographic image management was compliant with the Health Insurance Portability and Accountability Act.

CT scanning protocol. HRCT was used to scan patients at maximal inspiration. Images were acquired from 12 different multidetector CT scanner models from 2 manufacturers using a standardized procedure following strict quality control protocols. Most patients were scanned at suspended TLC in the prone position (n = 92 prone at both visits, n = 4 supine at baseline and prone at 24 months or vice versa, and n = 1 supine position at both visits). Tube currents ranged from 80 to 100 effective mAs at 120 kVp. Volumetric CT scans of 1–1.50-mm slice thickness were acquired and reconstructed with sharp or overenhancing filters. Ninety paired baseline and follow-up scans were acquired using the same CT scanner model.

Quantitative HRCT image analyses. *Quantitative CT image analysis*. Whole lung and individual lobes on HRCT images were segmented semiautomatically using an in-house analysis workstation (24). Visual confirmation of lobar segmentation results was performed by a thoracic radiologist.

Probability of changes in CT scores for extent of ILD abnormality during transition from one pattern of ILD to another. Quantitative CT texture-based scores of disease extent were derived from a supervised texture-based classification model (13). The following multistep process was used for generating voxelwise quantitative transitional probabilities from 97 paired HRCT scans: 1) classifying ILD patterns using a computer-aided diagnosis (CAD) system that automatically processes and reduces HRCT image noise, calculating the texture features, and running the support vector machine model (13); 2) registering (superimposing) the lobes and each lung between baseline and 24 months (24); 3) mapping each voxel (<27 mm^3) using a nearest-neighbor algorithm; and 4) counting the voxels within each mutually exclusive pattern of ILD (fibrosis, ground glass, honeycombing, and normal) at baseline and 24 months, and calculating a transitional probability (see Supplementary Figure 1 and Supplementary text, available on the *Arthritis & Rheumatology* web site at

for details of registration and transitional probability).

A transitional probability is an expression of the probability of changing from one radiographic pattern of ILD to another or retaining the same pattern, and is expressed as a proportion in which the numerator consists of the number of voxels representing a particular pattern of ILD that changes to another pattern (for example, a fibrotic pattern to a normal pattern) within a given region (whole lung or maximally involved lobe) between baseline and 24 months, and the denominator comprises the total number of voxels within the initial pattern at baseline. The probability of stability is the proportion of the number of voxels remaining in the same pattern at 24 months compared to baseline. A Markov transitional matrix schema was used to illustrate the probabilities of changes from one ILD pattern to another within the whole lung or the most severely affected lobe (25).

Four types of quantitative CT CAD patterns were computed: QLF, comprising a fibrotic reticulation pattern only; QHC, comprising a honeycomb pattern; QGG, comprising a ground-glass pattern; and QNL, representing normal lung patterns. Since only 2 of the 97 patients had a QHC >0 at baseline (one of 1.9% and the other of 5.3%) and the transitional probability of changing
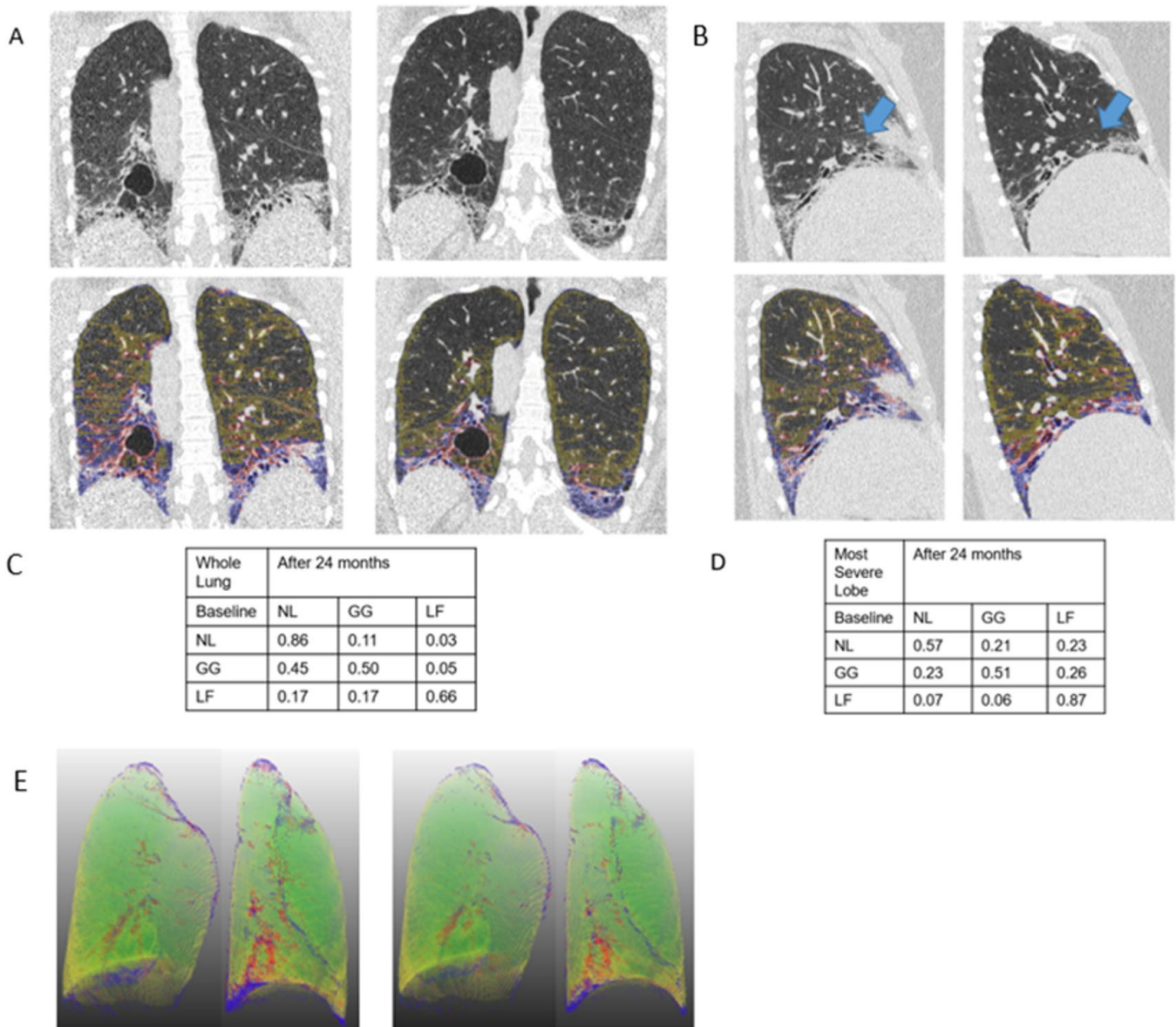
Figure 1. High-resolution computed tomography images of the lungs of a patient with systemic sclerosis–related interstitial lung disease (ILD) receiving cyclophosphamide. **A** and **B**, Coronal images of the whole lung (**A**) and sagittal images showing the right middle lobe (**blue arrows**) (**B**) obtained at baseline (left) and 24 months (right). Red and blue indicate quantitative lung fibrosis (LF); dark yellow indicates quantitative ground glass (GG). The remainder of the parenchymal area shows a quantitative normal (NL) lung pattern. **C** and **D**, Matrices showing transitional probabilities of change in ILD pattern in the whole lung (**C**) and the most severely affected lobe (the lower left lobe) (**D**). **E**, Three-dimensional rendering of coronal images showing normal lung pattern (green), quantitative lung fibrosis (blue and red), and a ground-glass pattern (yellow).

Table C:

Whole Lung	After 24 months		
Baseline	NL	GG	LF
NL	0.86	0.11	0.03
GG	0.45	0.50	0.05
LF	0.17	0.17	0.66

Table D:

Most Severe Lobe	After 24 months		
Baseline	NL	GG	LF
NL	0.57	0.21	0.23
GG	0.23	0.51	0.26
LF	0.07	0.06	0.87

from a honeycomb pattern to another pattern was 0, changes in a QHC pattern were omitted for simplicity and the 2 subjects with non-zero QHC scores were included in the QLF pattern under the assumption that honeycombing might represent a severe form of fibrosis. An example of a transitional probability from a lung fibrosis pattern to a ground-glass pattern is as follows: $P_{LF\,at\,baseline\,\rightarrow\,GG\,at\,follow-up}$ = counts of voxels that convert from LF to GG patterns/total number of voxels classified as LF at baseline. A stable voxelwise pattern was represented as $P_{NL\rightarrow NL}$, $P_{GG\rightarrow GG}$, or $P_{LF\rightarrow LF}$, indicating the probability of a normal, ground-glass, or fibrotic pattern, respectively, remaining the same over 2 years. A transitional net improvement was defined as the difference in 2 probabilities, in which the probability of a transition representing worsening (e.g., a ground-glass pattern transitioning to a fibrotic pattern) is subtracted from the probability of a transition representing improvement (e.g., a fibrotic pattern changing to a ground-glass pattern). Three net improvements were: $P_{GG\rightarrow NL} - P_{NL\rightarrow GG}$; $P_{LF\rightarrow NL} - P_{NL\rightarrow LF}$; and $P_{LF\rightarrow GG} - P_{GG\rightarrow LF}$.

Statistical analysis. Descriptive summary statistics were used for reporting demographic and clinical characteristics, pulmonary function measures, and quantitative CT texture scores at baseline and follow-up. CT scores are reported both for the whole lung and for the most severely affected lobe (the lobe with the greatest extent of disease as measured by the baseline QLF score) (26). We set up a 3 × 3 matrix consisting of the following transitions: diagonal elements representing stability ($P_{NL\rightarrow NL}$, $P_{GG\rightarrow GG}$, or $P_{LF\rightarrow LF}$) and off-diagonals representing transitional changes ($P_{LF\rightarrow GG}$, $P_{GG\rightarrow LF}$, $P_{GG\rightarrow NL}$, $P_{NL\rightarrow GG}$, $P_{LF\rightarrow NL}$, and $P_{NL\rightarrow LF}$) (Figures 1C and D). Net improvement between patterns is represented by the difference between 2 probabilities, e.g., the probability of transitioning from a lung fibrosis pattern to a normal lung pattern minus the probability of the directionally opposite transition, i.e., from a normal lung pattern to a lung fibrosis pattern ($P_{LF\rightarrow NL} - P_{NL\rightarrow LF}$).

After normality checks on a given metric, Wilcoxon's signed rank test was performed to test for the significance of net improvement from baseline (e.g., $P_{GG\rightarrow LF}$ versus $P_{LF\rightarrow GG}$ [difference in proportions between opposite directional patterns]) for the CYC and MMF groups separately. Spearman's rank correlations were used to test associations between changes in CT proportions in the whole lung and the most severely affected lobe and absolute changes in the percent predicted for pulmonary function test parameters. Linear regressions were used to determine the association of baseline demographic and clinical factors with the net benefit of change from ILD patterns of ground glass to normal and of lung fibrosis to normal. Backward selection methods were used with the covariates of age, sex, disease duration, pulmonary function, skin score, and dyspnea scores. A responder analysis was performed using +3% and –3.3% absolute changes in FVC% as the thresholds for defining responders and nonresponders, respectively. These thresholds represent previously published

findings for the minimal clinically important differences for absolute changes in FVC% anchored to health-related outcomes (27). Analysis of variance tests were used to compare the net improvements between the responder, stable, and nonresponder groups.

RESULTS

Baseline characteristics. Baseline demographic, lung function, clinical, and quantitative radiographic characteristics (the extent of fibrosis and total ILD in the whole lung and the lobe of maximal involvement) are shown in Supplementary Table 1, available on the *Arthritis & Rheumatology* web site at http://online library.wiley.com/doi/10.1002/art.41085/abstract. Patients (n = 47 in the CYC group and 50 in the MMF group) were predominantly women (74% [72 of 97]), were mostly middle-aged (mean ± SD 52 ± 9 years), and had, on average, moderate restrictive ventilatory and diffusion impairment (mean ± SD FVC% 66 ± 9% and DLco% 55 ± 13%, respectively) and a moderate level of breathlessness (mean ± SD BDI 7.5 ± 2.3). The mean ± SD MRSS was 14 ± 10, the extent of fibrosis was 23 ± 21%, and the extent of total ILD (fibrosis + ground glass + honeycombing) in the most severely involved lobe was 50 ± 22%.

Transitional proportion change. The mean ± SD duration between the baseline and follow-up CT scans was 24.6 ± 1.9 months. Figure 1 depicts an example of paired HRCT scans and overlaid images of quantitative patterns with 2 transitional matrices, one for the whole lung and the other for the most severely affected lobe (defined as the maximally involved lobe at baseline).

The mean transitional probability of change from each normal or ILD pattern (normal lung, ground glass, and lung fibrosis) to another pattern (e.g., from normal lung to ground glass; $P_{NL\rightarrow GG}$) or for remaining in the same pattern (e.g., from normal lung to normal lung; $P_{NL\rightarrow NL}$) for the whole lung and the most severely affected lobe is shown by treatment group in Table 1. There were no significant differences in transitional probabilities of change in ILD pattern between the 2 treatment groups ($P = 0.52$ for whole lung and $P = 0.47$ for the most severely affected lobe). Net improvements in ground-glass and fibrotic reticulation patterns, determined by subtracting unfavorable transitional probabilities from favorable ones (e.g., $P_{LF\rightarrow GG} - P_{GG\rightarrow LF}$), are shown in Table 2.

For the CYC group, mean transitional probabilities in the whole lung were as follows: 15% from fibrotic reticulation to ground glass ($P_{LF\rightarrow GG}$) and 10% from ground glass to fibrotic reticulation ($P_{GG\rightarrow LF}$) (Table 1), resulting in a net improvement ($P_{LF\rightarrow GG} - P_{GG\rightarrow LF}$) of 5% (Table 2); 25% from fibrotic reticulation to a normal pattern ($P_{LF\rightarrow NL}$), and 4% from a normal pattern to a fibrotic pattern ($P_{NL\rightarrow LF}$) (Table 1), with a net improvement ($P_{LF\rightarrow NL} - P_{NL\rightarrow LF}$) of 21% (Table 2); and 40% from a ground-glass pattern

Table 1. Probabilities of voxelwise transitions from one ILD pattern to another from baseline to 24 months by treatment assignment*

	CYC			MMF			Total		
	Normal	Ground glass	Lung fibrosis	Normal	Ground glass	Lung fibrosis	Normal	Ground glass	Lung fibrosis
Whole lung									
Baseline									
Normal	0.86 ± 0.02	0.10 ± 0.01	0.04 ± 0.01	0.88 ± 0.01	0.09 ± 0.01	0.03 ± <0.01	0.87 ± 0.01	0.10 ± 0.01	0.03 ± <0.01
Ground glass	0.40 ± 0.17	0.50 ± 0.15	0.10 ± 0.13	0.37 ± 0.02	0.51 ± 0.02	0.12 ± 0.02	0.38 ± 0.02	0.50 ± 0.01	0.11 ± 0.01
Lung fibrosis	0.25 ± 0.02	0.15 ± 0.02	0.60 ± 0.03	0.22 ± 0.02	0.12 ± 0.01	0.66 ± 0.03	0.24 ± 0.01	0.14 ± 0.01	0.62 ± 0.02
Most severely affected lobe									
Baseline									
Normal	0.76 ± 0.03	0.15 ± 0.02	0.09 ± 0.02	0.75 ± 0.03	0.14 ± 0.01	0.11 ± 0.0	0.75 ± 0.02	0.15 ± 0.01	0.10 ± 0.01
Ground glass	0.32 ± 0.03	0.52 ± 0.03	0.16 ± 0.03	0.28 ± 0.03	0.53 ± 0.02	0.19 ± 0.02	0.30 ± 0.20	0.53 ± 0.17	0.17 ± 0.02
Lung fibrosis	0.21 ± 0.03	0.16 ± 0.02	0.63 ± 0.04	0.18 ± 0.02	0.12 ± 0.02	0.70 ± 0.03	0.20 ± 0.02	0.14 ± 0.01	0.66 ± 0.02

* Values are the mean ± SEM. ILD = interstitial lung disease; CYC = cyclophosphamide; MMF = mycophenolate mofetil.

to a normal pattern ($P_{GG \to NL}$) and 10% from a normal pattern to a ground-glass pattern ($P_{NL \to GG}$) (Table 1), with a net improvement ($P_{GG \to NL} - P_{NL \to GG}$) of 30% (Table 2). For the MMF group, the net improvements in the whole lung were 0.5%, 19%, and 28% between fibrotic reticulation and ground-glass ($P_{LF \to GG} - P_{GG \to LF}$), between reticulation and a normal pattern ($P_{LF \to NL} - P_{LF \to NL}$), and between a ground-glass pattern and a normal pattern ($P_{GG \to NL} - P_{NL \to GG}$), respectively. Similar mean transitions were found in the most severely affected lobe (Table 1). There were no significant differences in the probability of 24-month change for total ILD between the 2 treatment groups ($P = 0.52$ for whole lung and $P = 0.47$ for the most severely affected lobe) (see Supplementary Table 2, available on the Arthritis & Rheumatology web site at http://onlinelibrary.wiley.com/doi/10.1002/art.41085/abstract).

The net improvements (or lack thereof) in the mean probabilities for these transitional changes for each treatment group separately and combined are also illustrated by box plots in Figure 2 and by the Markov transition chain schema in Figure 3. The findings demonstrate the mean net improvements in transitions from both lung fibrosis and a ground-glass pattern to a normal pattern in both treatment groups, but essentially no significant net improvement in transitions from lung fibrosis to a ground-glass pattern.

Table 3 shows the associations between quantitative CT changes (from baseline to 24-month follow-up) and both 1) baseline demographic and clinical/radiographic characteristics and 2) changes in clinical outcomes of lung function, dyspnea, and skin score over the same time period.

The clinical factors that were significantly associated with improvement from a ground-glass pattern to a normal pattern were high BDI scores (less baseline dyspnea) and female sex (adjusted $R^2 = 0.10$). Baseline clinical factors associated with favorable transitions from lung fibrosis to a normal pattern were less restrictive ventilatory impairment (less reduction in FVC), high (worse) skin scores, and female sex (adjusted $R^2 = 0.16$), by multivariate linear regression analysis.

Associations of transitional changes in ILD patterns with changes in relevant clinical features over 24 months are shown in the bottom portion of Table 3. The net improvements from a ground-glass pattern to a normal pattern and from fibrotic reticulation to a ground-glass pattern showed statistically significant correlations with all pulmonary function test measurements (% predicted FVC, DLco, and TLC) in both the whole lung and the most severely affected lobe, while improvement from a fibrotic pattern to a normal pattern

Table 2. Net improvement in ILD patterns based on voxelwise transitional changes*

Net improvement	Whole lung		Most severely affected lobe	
	CYC	MMF	CYC	MMF
$P_{GG \to NL} - P_{NL \to GG}$	0.30 ± 0.04†	0.28 ± 0.03†	0.17 ± 0.05‡	0.14 ± 0.03§
$P_{LF \to GG} - P_{GG \to LF}$	0.05 ± 0.03	0.005 ± 0.03	−0.006 ± 0.04	−0.07 ± 0.04
$P_{LF \to NL} - P_{NL \to LF}$	0.21 ± 0.02†	0.19 ± 0.02†	0.12 ± 0.04¶	0.07 ± 0.03#

* Net improvements were determined by subtracting unfavorable transitional probabilities (such as the probability of moving from a normal [NL] lung pattern to a ground-glass [GG] pattern [$P_{NL \to GG}$]) from favorable ones (such as the probability of moving from a ground-glass pattern to a normal lung pattern [$P_{GG \to NL}$]). Values are the mean ± SEM. ILD = interstitial lung disease; CYC = cyclophosphamide; MMF = mycophenolate mofetil; LF = lung fibrosis.
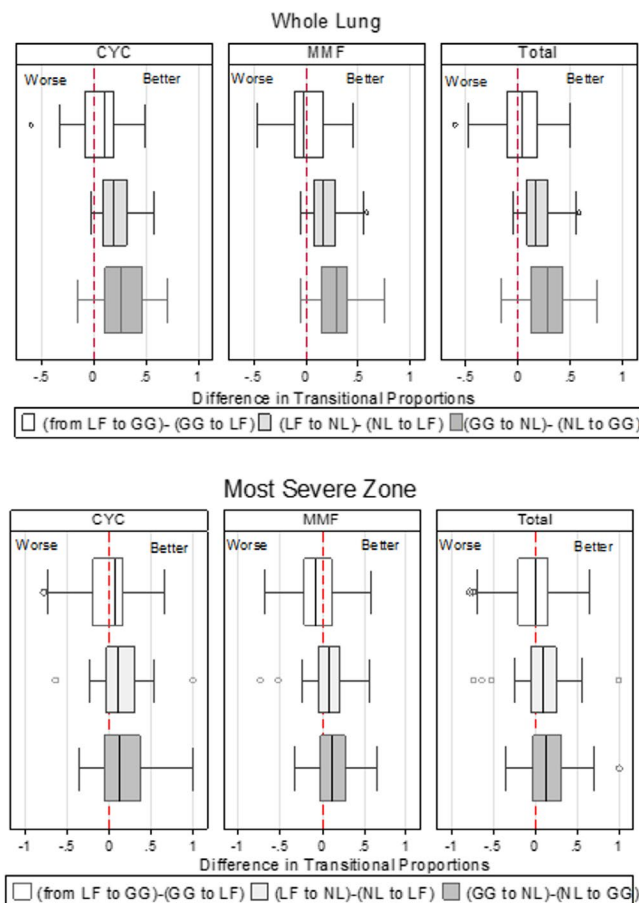† $P < 0.001$ versus a net improvement of 0.
‡ $P = 0.0008$ versus a net improvement of 0.
§ $P = 0.0384$ versus a net improvement of 0.
¶ $P = 0.0009$ versus a net improvement of 0.
# $P = 0.017$ versus a net improvement of 0.

Figure 2. Changes in interstitial lung disease (ILD) patterns in the whole lung (top) and most severely affected zone (bottom) in patients with systemic sclerosis–related ILD receiving cyclophosphamide (CYC), those receiving mycophenolate mofetil (MMF), and patients in both treatment groups combined. Patterns included lung fibrosis (LF), ground glass (GG), and normal lung (NL). Net improvements are expressed as the difference between 2 proportions ($P_{LF \to GG}$ − $P_{GG \to LF}$, $P_{LF \to NL}$ − $P_{NL \to LF}$, and $P_{GG \to NL}$ − $P_{NL \to GG}$). Data are shown as box plots, where the boxes indicate the interquartile range, lines inside the boxes indicate the median, and whiskers indicate 1.5 x (75th–25th percentile). Circles indicate outliers. Broken lines indicate no difference in the transitional changes. Color figure can be viewed in the online issue, which is available at http://onlinelibrary.wiley.com/doi/10.1002/art.41085/abstract.

was significantly associated with improvements in FVC and TLC in the whole lung only. Net improvements from fibrotic reticulation to both normal and ground-glass patterns in both the whole lung and the most severely affected lobe were also significantly correlated with favorable changes in skin score but not with the TDI. The net improvements from fibrotic reticulation to a ground-glass pattern and from fibrotic reticulation to a normal pattern showed significant correlations with changes in skin score in both the whole lung and the most severely affected lobe, whereas no significant associations were found between radiologic net improvement and changes in dyspnea.

A responder analysis was also performed to assess whether favorable transitional changes in ILD patterns were associated with clinically meaningful changes in FVC% using previously published values for minimal clinically meaningful differences in FVC% over a 1-year time period. Results of this analysis are shown in Supplementary Table 3, available on the *Arthritis & Rheumatology* web site at http://onlinelibrary.wiley.com/doi/10.1002/art.41085/abstract. Favorable transitional changes were uniformly greater in the responder and stable groups than in the nonresponder group, and differences across groups were significant, except for the transition from lung fibrosis to a normal pattern in the most severely affected lobe.

DISCUSSION

Treatment with either CYC for 1 year followed by placebo for an additional year, or with MMF for 2 years was associated with comparably significant increases in the probabilities of a net improvement from both ground-glass and fibrotic patterns of ILD to a normal lung pattern. Moreover, these favorable radiographic changes in the whole lung were associated with improvements in FVC and TLC, while the net improvement from a ground-glass to a normal pattern in both the whole lung and the most severely affected lobe was associated with improvements in DLco, FVC, and TLC. In addition, significant associations were found between the net improvement in fibrotic patterns and reduction in skin disease severity. These findings demonstrate that treatment-related improvements in structural patterns of ILD within the lung are accompanied by parallel improvements in lung function, as well as in extrapulmonary (cutaneous) involvement. Finally, transitional changes from a ground-glass pattern to a normal pattern, lung fibrosis to a ground-glass pattern, and lung fibrosis to a normal pattern were associated with minimal clinically important changes in FVC% that define either a positive response to immunosuppressive therapy or at least stable lung function.

Although specific baseline characteristics were significantly associated with favorable transitions from a ground-glass pattern to a normal pattern (less dyspnea and female sex) or from lung fibrosis to a normal pattern (less restriction, worse skin scores, and female sex), these associations, while significant, were not strong (adjusted R^2 0.10–0.16), underscoring the importance of clinical monitoring, including serial lung function measurements, along with judicious radiographic imaging.

This study provides further evidence that serial HRCT scans play an important and confirmatory role in monitoring the course of SSc-ILD. Patients with newly diagnosed SSc routinely undergo an initial HRCT scan as part of the assessment for the presence or absence of associated ILD with subsequent monitoring of lung function for evidence of the development or worsening of ILD (28). Follow-up HRCT scans may be warranted to confirm the development or worsening of ILD suggested by changes in lung function, given the variability and nonspecificity of lung function

Whole Lung

Most Severe Lobe
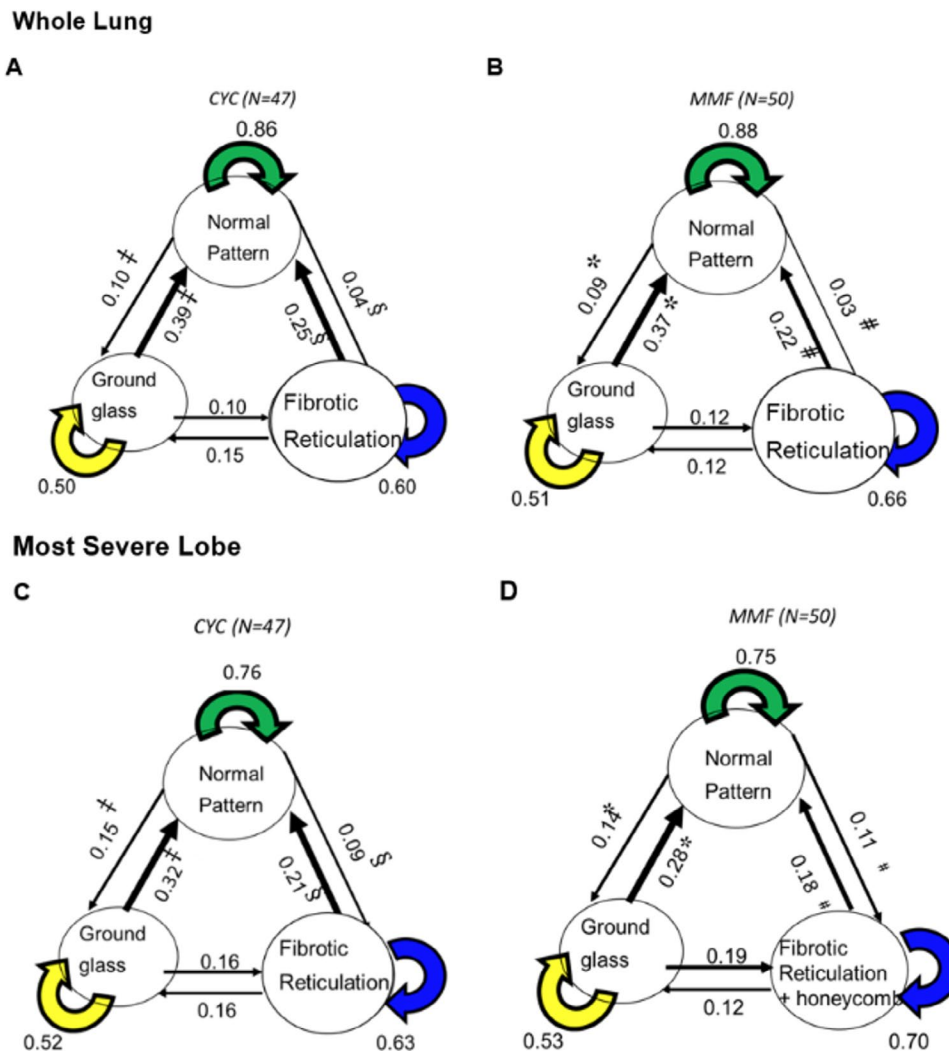
Figure 3. Schema of transitions in interstitial lung disease (ILD) patterns in patients with systemic sclerosis (SSc)–related ILD by treatment group. **A** and **B**, Transitions between patterns in the whole lung in patients treated with cyclophosphamide (CYC) (**A**) and patients treated with mycophenolate mofetil (MMF) (**B**). Values are the probability of transition. In **A**, ‡ = $P < 0.0001$ for improvement from a ground-glass (GG) pattern to a normal (NL) pattern; § = $P < 0.0001$ for improvement from lung fibrosis (LF) to normal; $P = 0.0568$ for improvement from lung fibrosis to a ground-glass pattern. In **B**, * = $P < 0.0001$ for improvement from a ground-glass pattern to normal; # = $P < 0.0001$ for improvement from lung fibrosis to normal; $P = 0.74$ for improvement from lung fibrosis to a ground-glass pattern. **C** and **D**, Transitions between patterns in the most severely affected lobe in patients treated with CYC (**C**) and patients treated with MMF (**D**). Values are the probability of transition. In **C**, ‡ = $P = 0.0008$ for improvement from a ground-glass pattern to normal; § = $P = 0.0009$ for improvement from lung fibrosis to normal; $P = 0.87$ for improvement from lung fibrosis to a ground-glass pattern. In **D**, * = $P = 0.0002$ for improvement from a ground-glass pattern to normal, # = $P = 0.017$ for improvement from lung fibrosis to normal; $P = 0.17$ for improvement from lung fibrosis to a ground-glass pattern. Color figure can be viewed in the online issue, which is available at http://onlinelibrary.wiley.com/doi/10.1002/art.41085/abstract.

measurements (which can be influenced by technical factors and/or inadequate patient effort [29,30]), in contrast to structural changes on HRCT that are more sensitive and specific indicators of parenchymal lung disease. The combination of lung function measurements and extent of ILD on HRCT has been suggested as a guide to decision-making regarding the initiation of disease-modifying therapy for SSc-ILD (16).

Continued monitoring of patients with established SSc-ILD already receiving immunosuppressive therapy with serial assessments of lung function and symptoms (e.g., dyspnea and cough)

may reveal equivocal findings (e.g., disparity between changes in lung function and dyspnea or between changes in FVC and DLco suggestive of pulmonary hypertension [31]) that might require a follow-up HRCT scan for definitive assessment regarding whether or not ILD has progressed, in which case a modification of the therapeutic regimen might be indicated. A recent publication of serial changes in lung function performed at 3-month intervals and follow-up HRCT scans in participants in SLS II provides some examples of patients with disparate changes in lung function and HRCT scans (32). Assessing the direction and magnitude of the quantitative

Table 3. Associations of transitional radiographic changes in ILD pattern with baseline characteristics and changes in lung function, skin score, and dyspnea*

| | Net improvement | | | | | |
| | Whole lung | | | Most severely affected lobe | | |
	$P_{GG→NL} - P_{NL→GG}$	$P_{LF→GG} - P_{GG→LF}$	$P_{LF→NL} - P_{NL→LF}$	$P_{GG→NL} - P_{NL→GG}$	$P_{LF→GG} - P_{GG→LF}$	$P_{LF→NL} - P_{NL→LF}$
Baseline						
Male, %	−0.26 (0.011)	−0.24 (0.02)	−0.15 (0.14)	−0.24 (0.018)	−0.23 (0.024)	−0.16 (0.12)
Age, years	0.12 (0.23)	−0.03 (0.74)	−0.09 (0.37)	0.15 (0.15)	−0.014 (0.89)	−0.06 (0.56)
Disease duration	−0.09 (0.37)	−0.11 (0.30)	−0.17 (0.10)	−0.17 (0.10)	−0.13 (0.19)	−0.10 (0.34)
FVC%	0.04 (0.69)	0.23 (0.021)	0.39 (0.0001)	0.08 (0.45)	0.31 (0.0024)	0.38 (0.0001)
FEV$_1$/FVC	−0.24 (0.017)	−0.15 (0.14)	−0.20 (0.052)	−0.16 (0.12)	−0.18 (0.077)	−0.17 (0.094)
DLco%	0.20 (0.0501)	0.23 (0.021)	0.33 (0.001)	0.24 (0.02)	0.25 (0.014)	0.30 (0.0025)
MRSS	−0.07 (0.48)	0.11 (0.21)	0.15 (0.14)	−0.03 (0.79)	0.10 (0.35)	0.10 (0.34)
BDI†	0.26 (0.011)	0.14 (0.20)	0.22 (0.03)	0.26 (0.012)	0.20 (0.049)	0.25 (0.014)
QLF, whole lung, %	−0.29 (0.0046)	−0.37 (0.0002)	−0.67 (<0.0001)	−0.32 (0.0013)	−0.49 (<0.0001)	−0.71 (<0.0001)
QILD, whole lung, %	−0.31 (0.0018)	−0.18 (0.07)	−0.46 (<0.0001)	−0.33 (0.0011)	−0.30 (0.0025)	−0.4881 (<0.0001)
QLF, most severely affected lobe, %	−0.30 (0.003)	−0.40 (0.0001)	−0.70 (<0.0001)	−0.36 (0.0003)	−0.53 (<0.0001)	−0.77 (<0.0001)
QILD, most severely affected lobe, %	−0.35 (0.0004)	−0.28 (0.0049)	−0.60 (<0.0001)	−0.43 (<0.0001)	−0.43 (<0.0001)	−0.69 (<0.0001)
24-month changes						
Change in FVC%	0.33 (0.0009)	0.45 (<0.0001)	0.21 (0.036)	0.3368 (0.0007)	0.4078 (<0.0001)	0.1787 (0.0798)
Change in DLco%	0.24 (0.022)	0.23 (0.028)	0.08 (0.43)	0.20 (0.050)	0.21 (0.042)	0.14 (0.17)
% change in TLC	0.28 (0.0059)	0.31 (0.002)	0.21 (0.042)	0.32 (0.0017)	0.29 (0.004)	0.14 (0.18)
% change in FEV$_1$/FVC	0.02 (0.88)	0.03 (0.74)	−0.03 (0.81)	0.00 (1.00)	0.11 (0.30)	0.05 (0.66)
Change in skin score‡	−0.107 (0.30)	−0.27 (0.0066)	−0.32 (0.0016)	−0.13 (0.19)	−0.25 (0.014)	−0.29 (0.0043)
TDI§	0.22 (0.059)	0.16 (0.19)	0.14 (0.25)	0.16 (0.18)	0.09 (0.46)	−0.0028 (0.98)

* Values are Spearman's rho (P). Net improvements were determined by subtracting unfavorable transitional probabilities (such as the probability of moving from a normal [NL] lung pattern to a ground-glass [GG] pattern [$P_{NL→GG}$]) from favorable ones (such as the probability of moving from a ground-glass pattern to a normal lung pattern [$P_{GG→NL}$]). ILD = interstitial lung disease; LF = lung fibrosis; FVC% = forced vital capacity % predicted; FEV$_1$ = forced expiratory volume in 1 second; DLco% = diffusing capacity for carbon monoxide % predicted; MRSS = modified Rodnan skin thickness score; QLF = quantitative lung fibrosis; QILD = quantitative interstitial lung disease (QLF + quantitative ground glass + quantitative honeycombing – quantitative normal lung pattern); TLC = total lung capacity.
† The Baseline Dyspnea Index (BDI) ranges from 0 (most severe) to 12 (unimpaired). Data were available for 89 patients.
‡ For changes in skin score a negative value represents improvement and a positive value represents worsening. Data were available for 97 patients.
§ For transition dyspnea index (TDI) a negative value represents worsening and a positive value represents improvement. Data were available for 72 patients.

voxelwise changes from one HRCT pattern of ILD to another represents a novel method of demonstrating the efficacy of treatment for SSc-ILD. This approach provides information on dynamic changes in the specific elements of structural abnormality of ILD patterns in the lung in response to treatment. This is both complementary to and more directly related to changes in abnormalities in lung structure than is the measurement of changes in lung function alone.

Interestingly, the net improvements in response to therapy that we noted were mainly from a fibrotic or a ground-glass pattern to a normal pattern, not from a fibrotic to a ground-glass pattern. While the pathobiology of ground-glass opacity in SSc-ILD is not clear (e.g., whether it represents inflammatory changes in the lung or early fibrosis), it is plausible that lung inflammation in SSc-ILD may be a precursor to fibrosis as the disease progresses.

Interpreting changes in quantitative ground-glass scores with regard to improvement or worsening in SSc-ILD is confounded by the fact that a ground-glass pattern can transition either to a normal pattern and/or another abnormal pattern (i.e., fibrosis) and that changes in the extent of the ground-glass pattern can occur by 4 different routes (normal→ground glass, ground glass→normal, ground glass→fibrosis, or fibrosis→ground glass). In SLS II, the probability of a ground-glass pattern remaining the same was relatively high in both treatment groups (0.50 for whole lung and 0.53 for the most severely affected lobe) (Table 1), but this "stability" appeared to be due to a combination of changes from other patterns of ILD to a ground-glass pattern, as well as concomitant transitions from ground-glass patterns to other patterns. Nonetheless, the clinically important findings were not transitions from lung fibrosis to a ground-glass pattern, but rather the net improvement in response to immunosuppressive therapy was reflected by transitions from either lung fibrosis or a ground-glass pattern to a normal pattern. In addition, these findings indirectly support using reductions in total ILD (lung fibrosis + ground glass + honeycombing) as an indication of treatment response in contrast to reductions in ground glass or fibrosis alone (33).

Our findings of a relatively high probability of lung fibrosis transitioning to a normal pattern (compared to the reverse) (0.24 for whole lung and 0.20 for the most severely affected lobe) (Table 1) are consistent with the previously reported radiographic results in SLS I, in which similar probabilities for these transitions in those receiving CYC were observed (0.19 for whole lung and 0.19 for the most severely affected zone) (20). Therefore, using two different approaches for quantifying the extent of different patterns of ILD, namely, voxelwise mapping of volumetric scans in SLS II and pixelwise hierarchical mapping using quantitative scores of 2-dimensional scans in SLS I, provided confirmatory findings with regard to the partial resolution of lung fibrosis in response to immunosuppressive therapy.

On the other hand, numerically higher probabilities were found in the transitions from a ground-glass pattern to a normal pattern in the CYC group in SLS II (Table 1) compared to the CYC group in SLS I (0.40 versus 0.14, respectively, in the whole lung and 0.32 versus 0.09, respectively, in the most severely affected lobe and zone at baseline) (20). This difference might be attributable to the differences between SLS II and SLS I in study populations, radiographic techniques (CAD classifier with voxelwise versus pixelwise quantitative scores and segmentation into lobes versus arbitrarily defined zones), and duration of follow-up (2 years versus 1 year).

In calculating the probability of these voxelwise transitional changes, we used a new metric, namely "net improvement" (the results of which are presented in Table 2) to counter potential measurement error in the registration of the 2 paired HRCT images due to a misalignment in voxels, which could potentially occur in the measurement of both favorable and unfavorable changes. Thus, using the difference between 2 transitional probabilities would be expected to reduce the impact of possible misalignment from registration.

It is noteworthy that both treatment groups in SLS II demonstrated relatively high probabilities of transitioning from either fibrosis or a ground-glass pattern to a normal lung pattern compared with changes in the reverse direction. These observations provide further support for the efficacy of both CYC and MMF in the management of symptomatic SSc-ILD, consistent with the favorable physiologic and patient-centered findings of SLS II, as previously described (21). These transitional changes may also provide insights into the pathobiology underlying responses to therapy for SSc-ILD. For example, it is possible that the changes from a ground-glass pattern to a normal pattern might represent complete resolution of fine, relatively loosely packed collagen fibrils, while the changes from a fibrotic to a normal pattern suggest that even coarser, more densely packed collagen is capable of complete resolution. The probability we observed of a net improvement from a fibrotic to a ground-glass pattern was close to 0, implying that the partial resolution of fibrosis in both SLS II and SLS I is reflected predominantly by a transition directly to a normal lung pattern rather than by an intermediate pathway wherein coarse fibrosis transitions to a finer subresolution type of fibrotic pattern represented by ground glass. However, it is possible that concomitant changes from a ground-glass pattern to a normal pattern may have obscured this intermediate step in the resolution of frank fibrosis.

The results of our analysis should be interpreted within the context of certain limitations. First, the voxelwise registration between 2 HRCT scans obtained 2 years apart can be confounded by measurement variation. Second, the metric of probability of changes does not capture the *absolute* extent of the difference in scores for the different patterns (QLF, QGG, or QHC), although it does capture the *directional* and proportional changes from baseline within these patterns of ILD. Third, while this metric of the probability of transitional changes in ILD patterns pertains to responses to immunotherapy for SSc-ILD mainly at the group level, its potential usefulness in the assessment and management of individual patients requires further study. Fourth, as with any sensitive computer-aided diagnostic system, standardization, quality control of scanning equipment, and methodologies regarding acquisition techniques such as reconstruction kernel, slice thickness, and safe and diagnostic levels of radiation are vitally important. Last, the transitional changes in ground glass and fibrotic reticulation based on the computer-aided classifier model using HRCT lack external validation by tissue histopathology.

Using voxel-by-voxel transitional scores on paired HRCT scans obtained 24 months apart during which patients with SSc-ILD were treated with MMF for the full 2 years or CYC for 1 year followed by placebo, we observed changes in the extent of ILD patterns indicating comparably significant net transitions from both fibrotic reticulation and ground-glass opacity to a normal lung pattern. These results imply partial resolution of both coarse and fine fibrosis and support and extend previous findings demonstrating improvement in lung function and clinical end points in response to treatment with MMF or CYC for SSc-ILD. These findings also demonstrate that voxelwise changes in ILD patterns of serial HRCT scans may be useful in monitoring the response to treatment of SSc-ILD when other data are inconclusive and provide potential insights into the nature of the therapeutic effects of these two immunosuppressive agents.

AUTHOR CONTRIBUTIONS

All authors were involved in drafting the article or revising it critically for important intellectual content, and all authors approved the final version to be published. Dr. Kim had full access to all of the data in the study and takes responsibility for the integrity of the data and the accuracy of the data analysis.
Study conception and design. Kim, Tashkin, Brown, Volkmann, Gjertson, Khanna, Elashoff, Tseng, Roth, Goldin.

Acquisition of data. Kim, Tashkin, Lo, Brown, Volkmann, Elashoff, Goldin.
Analysis and interpretation of data. Kim, Tashkin, Lo, Volkmann, Gjertson, Khanna, Elashoff, Tseng, Roth, Goldin.

REFERENCES

1. Abraham DJ, Varga J. Scleroderma: from cell and molecular mechanisms to disease models. Trends Immunol 2005;26:587–95.

2. Hachulla E, Launay D, de Groote P, Moranne O, Tillie-Leblond I, Seguy D, et al. Les défaillances viscérales graves de la sclérodermie systémique. Réanimation 2005;14:576–86.

3. Solomon J, Olson AL, Fischer A, Bull T, Brown KK, Raghu G. Scleroderma lung disease. Eur Respir Rev 2014;22:6–19.

4. Strollo D, Goldin J. Imaging lung disease in systemic sclerosis. Curr Rheumatol Rep 2010;12:156–61.

5. Steen VD, Conte C, Owens GR, Medsger TA Jr. Severe restrictive lung disease in systemic sclerosis. Arthritis Rheum 1994;37:1283–9.

6. Hansell DM, Bankier AA, MacMahon H, McLoud TC, Müller NL, Remy J. Fleischner Society: glossary of terms for thoracic imaging. Radiology 2008;246:697–722.

7. Kazerooni EA, Martinez FJ, Flint A, Jamadar DA, Gross BH, Spizarny DL, et al. Thin-section CT obtained at 10-mm increments versus limited three-level thin-section CT for idiopathic pulmonary fibrosis: correlation with pathologic scoring. AJR Am J Roentgenol 1997;169:977–83.

8. Uppaluri R, Hoffman EA, Sonka M, Hartley PG, Hunninghake GW, McLennan G. Computer recognition of regional lung disease patterns. Am J Respir Crit Care Med 1999;160:648–54.

9. Chabat F, Yang GZ, Hansell DM. Obstructive lung diseases: texture classification for differentiation at CT. Radiology 2003;228:871–7.

10. Zavaletta VA, Bartholmai BJ, Robb RA. High resolution multidetector CT-aided tissue analysis and quantification of lung fibrosis. Acad Radiol 2007;14:772–87.

11. Kim HJ, Li G, Gjertson D, Elashoff R, Shah SK, Ochs R, et al. Classification of parenchymal abnormality in scleroderma lung using a novel approach to denoise images collected via a multicenter study. Acad Radiol 2008;15:1004–16.

12. Iwasawa T, Asakura A, Sakai F, Kanauchi T, Gotoh T, Ogura T, et al. Assessment of prognosis of patients with idiopathic pulmonary fibrosis by computer-aided analysis of CT images. J Thorac Imaging 2009;24:216–22.

13. Kim HJ, Tashkin DP, Clements PJ, Li G, Brown MS, Elashoff R, et al. A computer-aided diagnosis system for quantitative scoring of extent of lung fibrosis in scleroderma patients. Clin Exp Rheumatol 2010;28 Suppl 62:S26–35.

14. Arzhaeva Y, Prokop M, Murphy K, van Rikxoort EM, de Jong PA, Gietema HA, et al. Automated estimation of progression of interstitial lung disease in CT images. Med Phys 2010;37:63–73.

15. Marten K, Dicken V, Kneitz C, Höhmann M, Kenn W, Hahn D, et al. Interstitial lung disease associated with collagen vascular disorders: disease quantification using a computer-aided diagnosis tool. Eur Radiol 2009;19:324–32.

16. Goh NS, Desai SR, Veeraraghavan S, Hansell DM, Copley SJ, Maher TM, et al. Interstitial lung disease in systemic sclerosis: a simple staging system. Am J Respir Crit Care Med 2008;177:1248–54.

17. Leroy EC, Medsger TA Jr. Criteria for the classification of early systemic sclerosis. J Rheumatol 2001;28:1573–6.

18. Tashkin DP, Elashoff R, Clements PJ, Goldin J, Roth MD, Furst DE, et al. Cyclophosphamide versus placebo in scleroderma lung disease. N Engl J Med 2006;354:2655–66.

19. Roth MD, Tseng CH, Clements PJ, Furst DE, Tashkin DP, Goldin JG, et al, for the Scleroderma Lung Study Research Group. Predicting treatment outcomes and responder subsets in scleroderma-related interstitial lung disease. Arthritis Rheum 2011;63:2797–808.

20. Kim HJ, Tashkin DP, Gjertson DW, Brown MS, Kleerup E, Chong S, et al. Transitions to different patterns of interstitial lung disease in scleroderma with and without treatment. Ann Rheum Dis 2016;75:1367–71.

21. Tashkin DP, Roth MD, Clements PJ, Furst DE, Khanna D, Kleerup EC, et al. Mycophenolate mofetil versus oral cyclophosphamide in scleroderma-related interstitial lung disease (SLS II): a randomised controlled, double-blind, parallel group trial. Lancet Respir Med 2016;4:708–19.

22. Mahler DA, Tomlinson D, Olmstead EM, Tosteson AN, O'Connor GT. Changes in dyspnea, health status, and lung function in chronic airway disease. Am J Respir Crit Care Med 1995;151:61–5.

23. Clements PJ, Lachenbruch PA, Seibold JR, Zee B, Steen VD, Brennan P, et al. Skin thickness score in systemic sclerosis: an assessment of inter-observer variability in 3 independent studies. J Rheumatol 1993;20:1892–6.

24. Klein S, Staring M, Murphy K, Viergever MA, Pluim JP. Elastix: a toolbox for intensity-based medical image registration. IEEE Trans Med Imaging 2010;29:196–205.

25. Hoel PG, Port SG, Stone CJ. Introduction to stochastic processes. 1st ed. Prospect Heights (IL): Waveland Press Inc.; 1987. p. 12–29.

26. Kim HJ, Brown MS, Elashoff R, Li G, Gjertson DW, Lynch DA, et al. Quantitative texture-based assessment of one-year changes in fibrotic reticular patterns on HRCT in scleroderma lung disease treated with oral cyclophosphamide. Eur Radiol 2011;21:2455–65.

27. Kafaja S, Clements PJ, Wilhalme H, Tseng CH, Furst DE, Kim GH, et al. Reliability and minimal clinically important difference of forced vital capacity: results from the Scleroderma Lung Studies (SLS-I and SLS-II). Am J Respir Crit Care Med 2018;197:644–52.

28. Khanna D, Miltoo S, Aggarwal R, Proudman SM, Dalbeth N, Matteson EL, et al. connective tissue disease-associated interstitial lung diseases (CTD-ILD): report from OMERACT CTD-ILD Working Group. J Rheumatol 2015;42:2168–71.

29. Miller MR, Hankinson J, Brusasco V, Burgos F, Casaburi R, Coates A, et al. Standardisation of spirometry. Eur Respir J 2005;26:319–38.

30. Graham BL, Brusasco V, Burgos F, Cooper BG, Jensen R, Kendrick A, et al. 2017 ERS/ATS standards for single-breath carbon monoxide uptake in the lung. Eur Respir J 2017;49:1600016.

31. Galiè N, Humbert M, Vachiery JL, Gibbs S, Lang I, Torbicki A, et al. 2015 ESC/ERS guidelines for the diagnosis and treatment of pulmonary hypertension: the Joint Task Force for the Diagnosis and Treatment of Pulmonary Hypertension of the European Society of Cardiology (ESC) and the European Respiratory Society (ERS). Endorsed by: Association for European Paediatric and Congenital Cardiology (AEPC), International Society of Heart and Lung Transplantation (ISHLT). Eur Heart J 2009;37:67–119.

32. Volkmann ER, Tashkin DP, Sim M, Kim GH, Goldin JG, Clements PJ. Determining progression of scleroderma-related interstitial lung disease. J Scleroderma Relat Disord 2018;4:62–70.

33. Goldin JG, Kim GH, Tseng CH, Volkmann E, Furst D, Clements P, et al. Longitudinal changes in quantitative interstitial lung disease on computer tomography after immunosuppression in the Scleroderma Lung Study II. Ann Am Thorac Soc 2018;15:1286–95.